Case Studies in Thermal Engineering 27 (2021) 101334

Contents lists available at ScienceDirect

Case Studies in Thermal Engineering

journal homepage: www.elsevier.com/locate/csite

Numerical exploration of thermal transport in water-based nanoparticles: A computational strategy

Tahir Naseem [a], Umar Nazir [b], Muhammad Sohail [b,*], Hussam Alrabaiah [c,d], El-Sayed M. Sherif [e], Choonkil Park [f,**]

[a] Department of Mathematics, Government Postgraduate College Haripur, Pakistan
[b] Department of Applied Mathematics and Statistics, Institute of Space Technology, P.O. Box 2750, Islamabad, 44000, Pakistan
[c] College of Engineering, Al Ain University, Al Ain, United Arab Emirates
[d] Department of Mathematics, Tafila Technical University Tafila, Jordan
[e] Mechanical Engineering Department, College of Engineering, King Saud University, P.O. Box 800, Al-Riyadh, 11421, Saudi Arabia
[f] Research Institute for Natural Sciences, Hanyang University, Seoul, 04763, South Korea

ARTICLE INFO

Keywords:
Nanofluid
Bi-directional stretching sheet
Three-dimensional flow
MHD effect
Thermal conductivity
Heat transfer rate
Shooting method

ABSTRACT

This report examines the three-dimensional flow characteristics and heat transfer of TiO_2–Cu/water nanofluid past over a bidirectional surface with the effect of MHD. Tiwari and Das model of nanofluid is used with the thermophysical properties of nanofluid. The derived physical laws have been simplified under boundary layer theory. The complex sets of coupled PDEs have developed in form of ODEs by utilizing the appropriate transformations. The transformed equations handled via shooting method. The impacts of different influential parameters have been sketched. The involvement of different parameters for dimensionless stress, rate of heat and mass are tabulated. Limiting case of present investigation is compared with those of published ones and an excellent settlement is noted. It is noted that the enhancement in fluid parameters behave contrary to fluid velocity as compared with thermal and concentration profile. Moreover, thermal profile depreciate against higher values of Eckert and Prandtl numbers.

1. Introduction

Nano particles are used to enhance the thermal performance of systems which has numerous application and usage in different mechanisms. In the current era nanoparticles is the hot topic of research. Several researchers have worked on nanofluids, mass and thermal transportation. For instance, Marzougui et al. [1] studied the copper-water mixture nanofluid in a cavity. They studied the physical features and impact of numerous involved parameters by using the COMSOL tool. Also, they reported the computational analysis for entropy generation. Bhutta et al. [2] analyzed for the efficiency of multilayers SiO_2 films experimentally. They used the mechanisms of synthesis. Stability analysis and dual solution is examined for Williamson model containing titanium alloy by Khan et al. [3]. They solved the model equations numerically. They performed the comparative analysis. They reported that augmentation in volume fraction of nanoparticles enhanced the skin fraction coefficient and heat transportation rate for the dual solutions. Adelmalek et al. [4] studied the suspicious of hybrid nanoparticles in Carreau liquid by considering chemical reaction and heat generation

* Corresponding author.
** Corresponding author.
E-mail addresses: muhammad_sohail111@yahoo.com (M. Sohail), baak@hanyang.ac.kr (C. Park).

https://doi.org/10.1016/j.csite.2021.101334
Received 17 May 2021; Received in revised form 29 July 2021; Accepted 9 August 2021
Available online 13 August 2021

Nomenclature

Symbols/text	*Used for*
MBL	Momentum boundary layer
C_{fx}, C_{fy}	Skin friction
Pr	Prandtl number
M	Magnetic parameter
TBL	Thermal boundary layer
Nu	Nusselt number
Ec	Eckert number
c	Stretching velocity ratio

inspiration. They used the Galerkin scheme to handle the nonlinear transmuted system of differential equations. Vaidya et al. [5] scrutinized the phenomenon of mixed convection in nanofluid past over a Riga plate which is stretched nonlinearly. In their exploration, they deliberated the buoyancy opposing and assisting region. Shah et al. [6] studied the contribution of nanoparticles in chemically reactive based water model. They discussed the flow dynamics past over a stretching sheet. They established the comparative study for the authenticity of the solution and proposed scheme and found that the obtained solution is an excellent agreement to the existing one. Nawaz et al. [7] investigated the heat transport in hybrid nanoparticle mixture by using the Cattaneo-Christov theory. They consider the non-uniform magnetic field. They handled the flow presenting expressions via FEM. Nisar et al. [8] study the convection in squeezed flow dynamics in hybrid model between rotating disks. They plotted the flow dynamics for suction parameter via stream lines patterns. They noticed the rise in thermal profile against radiation parameter. Shafiq et al. [9] utilized the slip flow mechanism in Darcy-Forchheimer medium. Rotating flow dynamics with convective conditions are examined. They noticed the decline in velocity field against the up-surging values of magnetic parameter. Waqas et al. [10] studied the compartment of activation energy in thermal transport of Burger Bio convective nanofluid comprising gyrotactic microorganisms. They developed the boundary conditions by using the slip theory. BVP4C built in package in MATLAB is used to approximate the solution for converted nonlinear equations. They reported that higher estimation in bio convection Rayleigh number diminishes the mass diffusion. Sohail et al. [11] studied the involvement of temperature dependent diffusion coefficient and thermal conductivity for mass and thermal transmission in Sutterby model via OHAM. Dawar et al. [12] studied the involvement of momentum slip to investigate the transport phenomenon for micropolar fluid. Aldabesh et al. [13] studied the flow of nanofluid between parallel rotating disks. Brownian diffusion and thermopherosis effects are considered. They recorded that higher values of Biot number enhances the concentration field. Javed et al. [14] studied the involvement of chemical reactions in peristaltic flow under slip conditions in curved wavy channel. Slimani et al. [15] studied the natural convection in hybrid nanofluid model in a porous enclosure via finite element

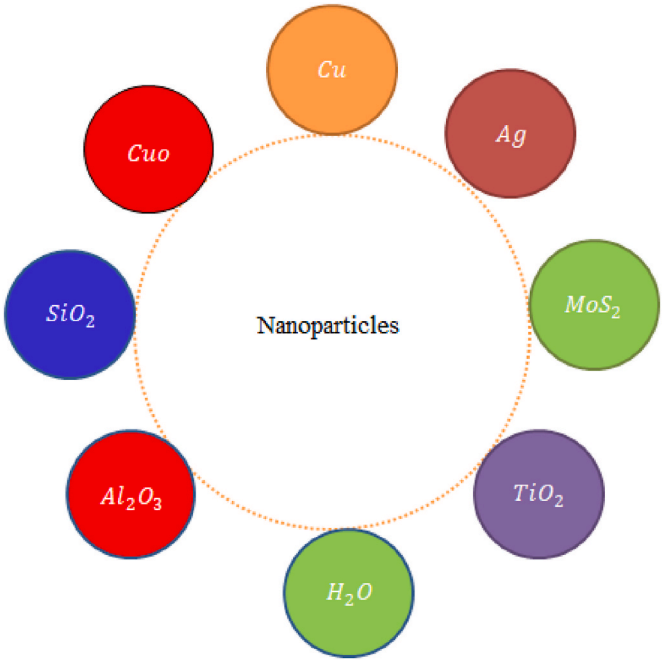

Fig. 1a. Sketched view of nanoparticles.

procedure. Zaydan et al. [16] discussed the transport phenomena in mixed convective flow. Shahzad et al. [17] studied the unsteady dynamics for axisymmetric flow in radially stretching surface. Sheikholeslami et al. [18] discussed an enhancement in heat energy related to flat plate solar collectors including the productivity of photovoltaic. They provided overview of solar water heating and critical economic systems. Sheikholeslami et al. [19] studied the thermal characteristics behavior of nanoparticles including towards solar collector plate. They also simulated the entropy generation along with nanoparticles. Several other researchers have attempted recently to discuss the dynamics of stretched flows as mentioned in Refs. [20–25].

Above cited explorations focus on thermal and mass transportation by using the traditional nanofluid model. Here, we extended the work of Khan et al. [20] by utilizing the famous Das and Tiwari nanofluid model by considering the different shape factors along with magnetrohydrodynamics effect. In this work, the diffusion of nanoparticles *Cu* and TiO_2 in base fluid called water is formulated as no work on heat energy including the effects of constant magnetic field and Joule heating phenomenon inserting the various kinds of shapes nanoparticles (Blade, Brick, Sphere, Platelets and Cylinder) is simulated yet. The formulation of heat transfer problem along with BCs (boundary conditions) is solved by shooting approach. The performed investigation is arranged as: Section I contains the literature survey, dynamics of fluid with important quantities are presented in Section II, Section III contains the solution methodology, physical aspects on obtained solution are detailed in Section IV and important findings are mentioned in Section V. The sketched view of various nanoparticles is assumed by Fig. 1 (a).

2. Mathematical formulation of transport problem

The three dimensional incompressible boundary layer flow of TiO_2-Cu/water nanofluid past over a bi-directional stretching surface by keeping the origin fixed is considered. It is further considered that the surface moves with velocities $u = U_w(x) = ax$ and $v = V_w(y) = by$, where $a, b > 0$ corresponds to the case of stretching along x- and y-directions respectively. The considered transport rheology is presented under boundary layer theory.

The considered physical happening is depicted by Fig. 1 (b). The arising problem in the form of coupled system of PDEs is

$$\frac{\partial u}{\partial x}+\frac{\partial v}{\partial y}+\frac{\partial w}{\partial z}=0, \tag{1}$$

$$u\frac{\partial u}{\partial x}+v\frac{\partial u}{\partial y}+w\frac{\partial u}{\partial z}=\nu_{nf}\frac{\partial^2 u}{\partial z^2}-\frac{\sigma_{nf}}{\rho_{nf}}B^2u, \tag{2}$$

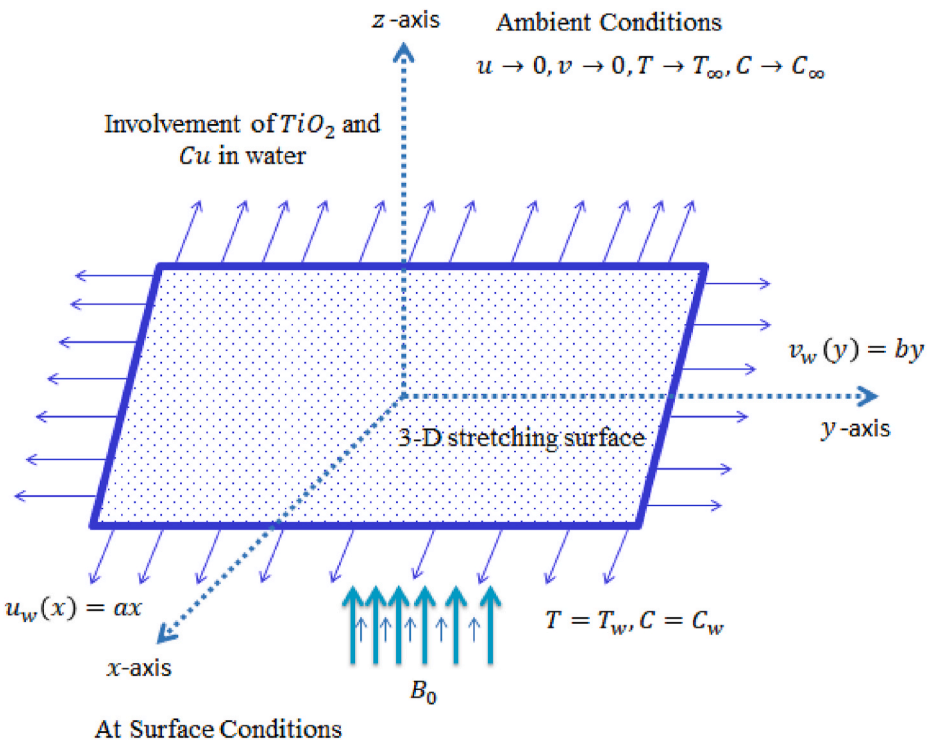

Fig. 1b. Flow phenomenon of fluid regarding space coordinates.

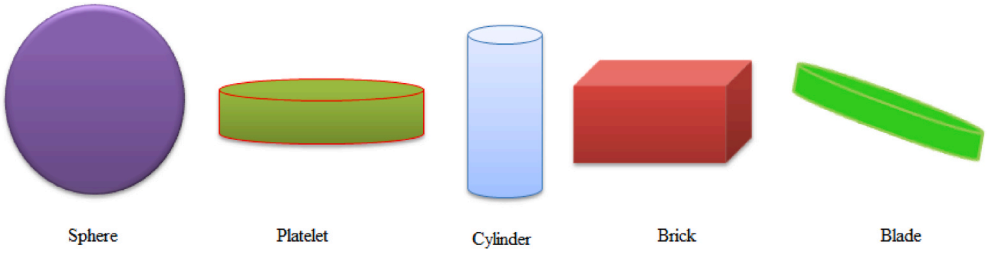

Fig. 1c. Geometrical view (size) of nanoparticles.

$$u\frac{\partial v}{\partial x}+v\frac{\partial v}{\partial y}+w\frac{\partial v}{\partial z}=\nu_{nf}\frac{\partial^2 v}{\partial z^2}-\frac{\sigma_{nf}}{\rho_{nf}}B^2 v, \tag{3}$$

$$u\frac{\partial T}{\partial x}+v\frac{\partial T}{\partial y}+w\frac{\partial T}{\partial z}=\alpha_{nf}\frac{\partial^2 T}{\partial z^2}+\frac{\mu_{nf}}{(\rho Cp)_{nf}}B_0{}^2 u\left(\frac{\partial u}{\partial y}\right)^2, \tag{4}$$

where density, viscosity, thermal diffusivity, and electrical conductivity of nanofluid respectively are denoted as: $\rho_{nf}=(1-\varphi)\rho_f+\varphi\rho_s$, $\mu_{nf}=\mu_f(1+A^1\varphi+A^2\varphi^2), \alpha_{nf}=\frac{k_{nf}}{(\rho Cp)_{nf}}$.

The thermal conductivity ratio is given by: $\frac{k_{nf}}{k_f}=\frac{k_s+(m-1)k_f+(m-1)(k_s-k_f)\varphi}{k_s+(m-1)k_f-(k_s-k_f)\varphi}$, where $\varphi, k_{nf}, (\rho Cp)_{nf}$, and A^1, A^2 are respectively the volume fraction, thermal conductivity, heat capacitance and viscosity enhancement coefficients of the nanofluid whereas k_s and m are thermal conductivity and shape factor nanoparticles and their values are mentioned in Table 2. Geometrical view (size) of nanoparticles is captured by Fig. 1 (c).

The numerical shape factor and viscosity enhancement coefficients are given in Table 1.

The corresponding BCs subjected to fluid flow are

$$\left.\begin{array}{l} u=U_w(x)=ax,\ T=T_w,\ v=V_w(y)=by,\\ w=0, \end{array}\right\}\text{at } z=0, \tag{5}$$

$$u\to 0,\ v\to 0,\ T\to T_\infty,\ \text{as } z\to\infty. \tag{6}$$

Considering the following similarity transformations

$$u=axf'(\eta),\ v=byg'(\eta), w=-\sqrt{av_f}(f(\eta)+cg(\eta)), \tag{7}$$

$$\eta=\sqrt{\frac{a}{v_f}}z,\ \theta(\eta)=\frac{T-T_\infty}{T_w-T_\infty}, c=\frac{b}{a}, \tag{8}$$

Using Eqs. (7) and (8), in Eqs. (1)–(6), Eq. (1) is identically satisfied, while the governing Eqs. (2)–(6) becomes

$$\varepsilon_1 f'''+(f+g)f''-(f')^2-M\varepsilon_3 f'=0, \tag{9}$$

$$\varepsilon_1 g'''+(f+g)g''-(g')^2-M\varepsilon_3 g'=0, \tag{10}$$

$$\varepsilon_2\,\theta''+Pr(f+g)\theta'+Ec(f'')^2=0, \tag{11}$$

$$f(0)=0,\ f'(0)=1,\ g(0)=0,\ g'(0)=c,\ \theta(0)=1,\ f'(\infty)\to 0,\ g'(\infty)\to 0,\ \theta(\infty)\to 0. \tag{12}$$

Table 1
Viscosity coefficient and shape factor corresponding five different shapes of nanoparticles.

Nanoparticle Shapes	A^1	A^2	Shape factors (m)
Blade	14.6	123.3	8.26
Brick	1.9	471.4	3.72
Cylinder	13.5	904.4	4.82
Platelets	37.1	612.6	5.72
Sphere	2.5	6.5	3.0

Table 2
Thermophysical properties of two nanoparticles and water.

Nanoparticles/Base fluid	*Cu*	TiO_2	H_2O
$\rho(kg.m^{-3})$	8933	4250	997.1
$Cp(J.kg^{-1}.K^{-1})$	385	686.2	4179
$k(W.m^{-1}.K^{-1})$	401	8.9538	0.613
$\sigma(\Omega^{-1}.m^{-1})$	59.6	0.125	5.5

2.1. Physical quantities

The thermo-physical parameters in equations (9 −11) dictating the flow dynamics and are defined as

$$Pr=\frac{\nu}{\alpha_{nf}}, c=\frac{a}{b}, Ec=\frac{U^2}{Cp(T_s-T)}, \text{ and } M=\frac{\sigma_f {B_0}^2}{\rho_{nf} b}. \tag{13}$$

Finally, ε_1, ε_2, and ε_3 are constants which are defined by

$$\varepsilon_1=\frac{\left(1+A^1\varphi+A^2\varphi^2\right)}{\left(1-\varphi+\varphi\frac{\rho_s}{\rho_f}\right)},\ \varepsilon_2=\frac{\frac{K_{nf}}{K}}{1-\varphi+\varphi\frac{(\rho Cp)_s}{(\rho Cp)_f}}, \varepsilon_3=\frac{1-\varphi+\varphi\frac{\sigma_s}{\sigma_f}}{1-\varphi+\varphi\frac{\rho_s}{\rho_f}}. \tag{14}$$

The dimensionless expression of the local skin-friction coefficient, and the local Nusselt number, respectively are

$$\begin{cases} C_{fx}=\dfrac{2\mu_{nf}\left(\dfrac{\partial u}{\partial z}\right)_{z=0}}{\rho_f U^2}=Re^{-\frac{1}{2}}\left(1+A^1\varphi+A^2\varphi^2\right)f''(0), \\ C_{fy}=\dfrac{2\mu_{nf}\left(\dfrac{\partial v}{\partial z}\right)_{z=0}}{\rho_f U^2}=Re^{-\frac{1}{2}}\left(1+A^1\varphi+A^2\varphi^2\right)g''(0) \\ Nu=\dfrac{-xK_{nf}\left(\dfrac{\partial T}{\partial z}\right)_{z=0}}{T_s-T_0}=Re^{\frac{1}{2}}\dfrac{K_{nf}}{K}\theta'(0). \end{cases}, \tag{15}$$

2.2. Numerical method for solution

The transformations have played a character for achievement regarding the system of ODEs from the system of PDEs. The derived flow model (ODEs) involving BCs are solved by using Shooting method. Here, the dimensionless third order (ODEs) (9 −10) and second order (ODEs) (11) have been reduced to first order differential equations. The system of ODEs within BCs (boundary conditions) is known as couple and non-linear in nature. The shooting approach is implemented to compute solution of required ODEs. Firstly, linear DEs (differential equations) are made considering below

$$f=y_1, f'=y_2, f''=y_3,\ g=y_4, g'=y_5, g''=y_6, f'''=\frac{1}{\varepsilon_1}\left[-(y_1+y_4)y_3+(y_2)^2+M\varepsilon_3 y_2\right], \tag{16}$$

$$g'''=\frac{1}{\varepsilon_1}\left[-(y_1+y_4)y_6+(y_5)^2+M\varepsilon_3 y_5\right]=0, \tag{17}$$

$$\theta=y_7, \theta'=y_8,\ \theta''=\frac{1}{\varepsilon_2}\left[-Pr(y_1+y_4)y_8-Ec(y_3)^2\right], \tag{18}$$

and corresponding boundary condition becomes

$$y_1(0)=0,\ y_2(0)=1,\ y_4(0)=0,\ y_5(0)=c, y_7(0)=1, y_2(\infty)=0,\ y_5(\infty)=0,\ y_7(\infty)=0\,. \tag{19}$$

The set of equations (16 −18) subject to boundary conditions (19) are solved using the proposed technique. The computation has been carried out by using MATLAB. The iterative process will be terminated up to the desired degree of accuracy (10^{-6}) is obtained. The iterative approach is used to simulate BCs (boundary conditions) and iterative approach is also known as shooting scheme. The related code is designed on MATLAB whereas code is successfully implemented to compute wide range transport phenomena related problems. The criterion related convergence of problem is considered as 10^{-6}. In this approach, it is noticed that the value of η_∞ is adjusted according to graphical behavior.

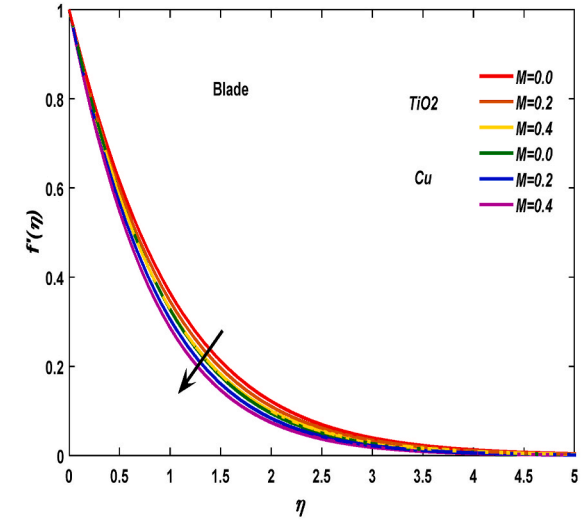

(a)

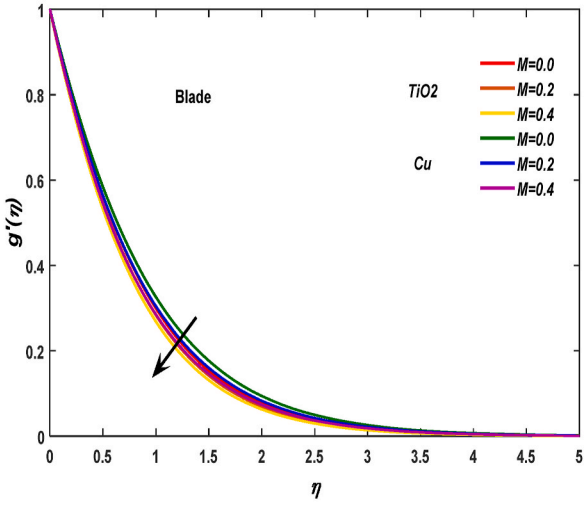

(b)

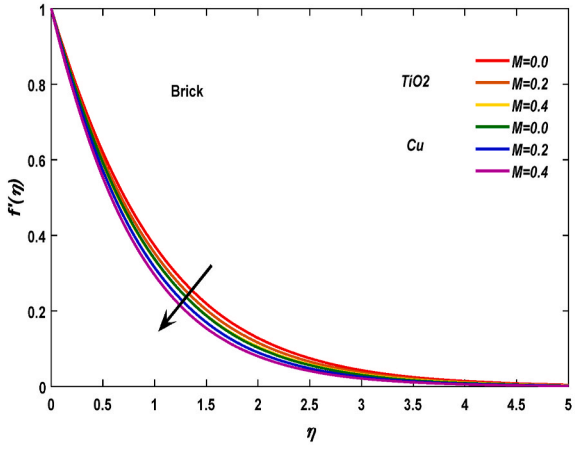

(c)

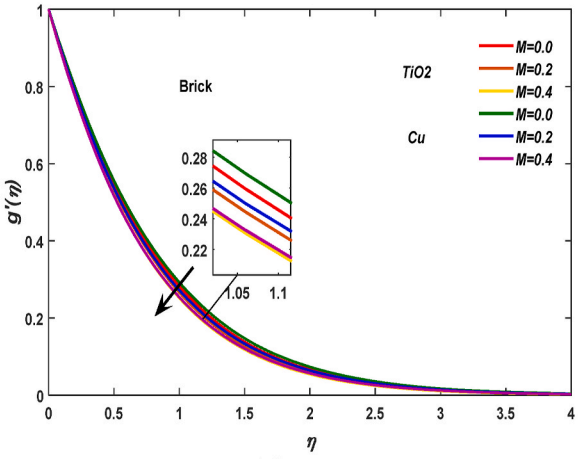

(d)

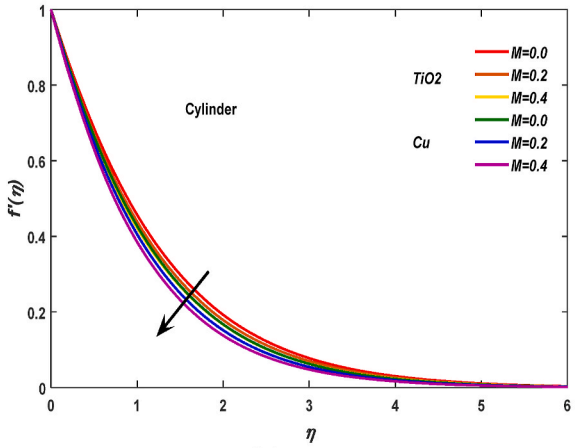

(e)

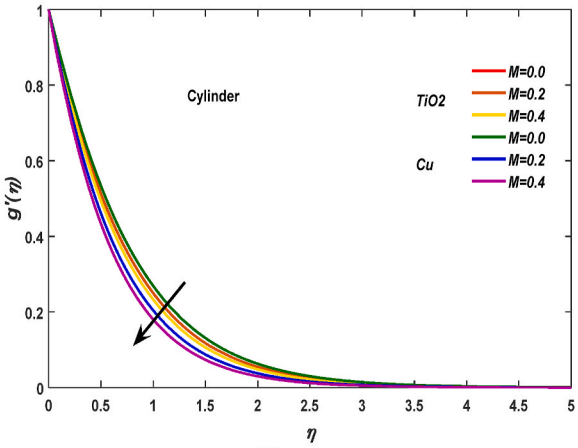

(f)

Fig. 2. (a–j). Variation of M on $(f^{'}, g^{'})$ by using different shape nanoparticles.

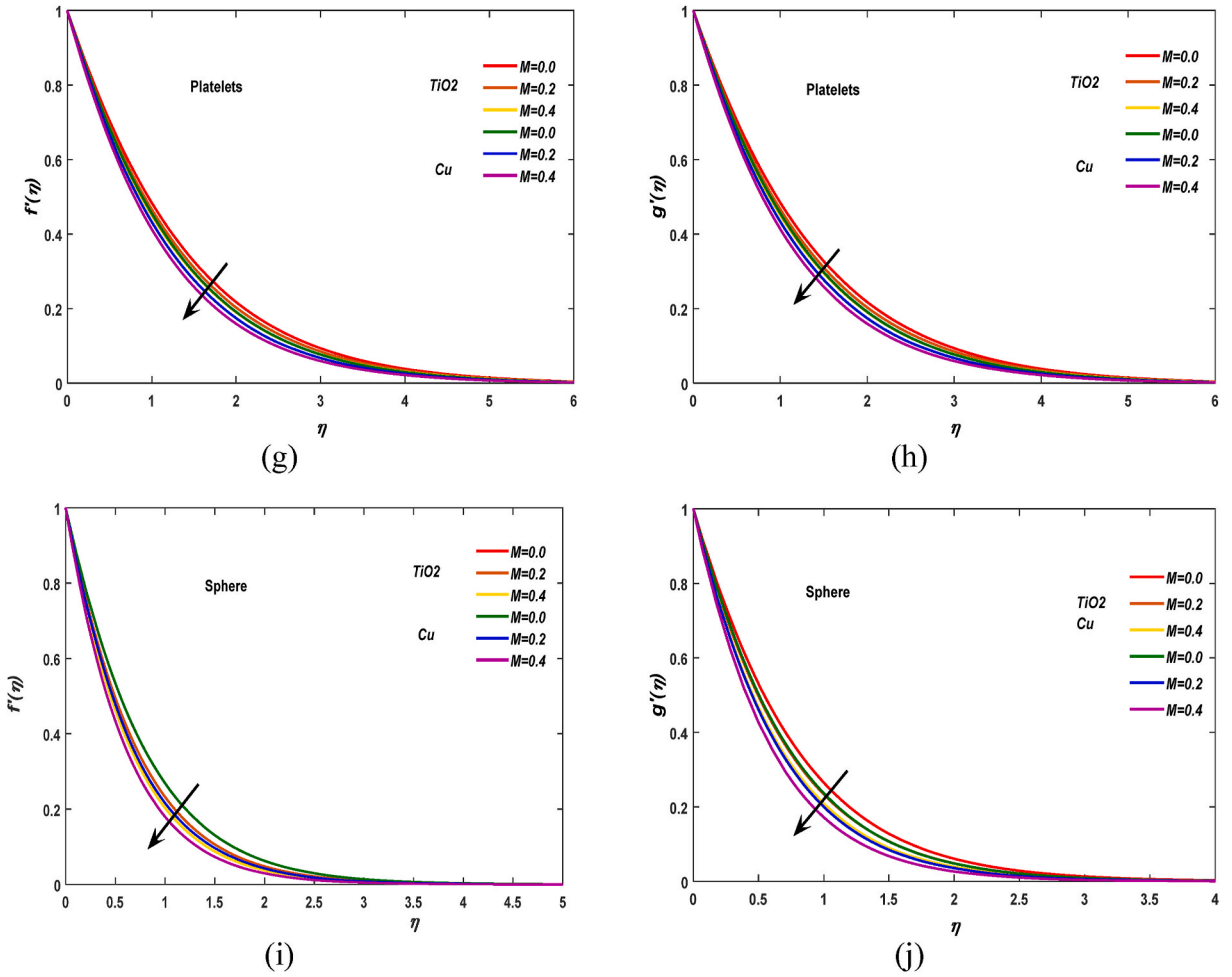

Fig. 2. (*continued*).

4. Results and discussion

Three directional and three dimensional thermal energy transport phenomenon in Newtonian fluid involving the role of magnetic field and heat dissipation while various shapes of nanoparticles (Blade, Brick, Cylinder, Platelets and Sphere) in view of *Cu* and TiO_2 nanoparticles are incorporated in base fluid called water over a moving surface. This transport phenomenon of thermal energy is conducted by numerical technique. The description regarding velocity and temperature versus various parameters is conducted through graphs and tables whereas related description of this flow model is given below.

Comparative study of TiO_2 and *Cu* in view of velocity field: The flow phenomenon in view of Blade, Brick, Cylinder, Platelets and Sphere shapes nanoparticles is suspended with *Cu* and TiO_2 nanoparticles versus magnetic field, stretching ratio number and volume fraction. The role of magnetic number (M) on the flow of *Cu* and TiO_2 nanoparticles in view of Blade, Brick Platelets and Sphere shapes nanoparticles are simulated by Fig. 2a, b, 2c, 2d, 2e, 2f, 2g, 2h,2i, and 2j. From these figures, it is investigated that flow of *Cu* and TiO_2 nanoparticles becomes slow down because magnetic number is appeared due to Lorentz force. Further, negative Lorentz force makes a vital role for making more friction in flow of *Cu* and TiO_2 nanoparticles. It is noticed that Lorentz force is known as opposing force in direction of flow phenomena. The direction of magnetic field is considered normal to flow of nanoparticles. Hence, flow is reduced. Therefore, flow of *Cu* and TiO_2 nanoparticles becomes slowdown in the presence of Blade, Brick Platelets and Sphere shapes nanoparticles. From these figures, it also simulated that flow in term of TiO_2-nanofluid is higher than flow in term of *Cu*-nanofluid while TiO_2-nanofluid is used for more enhancement of heat transfer and higher flow as compared to *Cu*-nanofluid. Magnetic number plays important role for manage the flow phenomena in presence of Blade, Brick Platelets and Sphere shapes nanoparticles including *Cu* and TiO_2 nanoparticles. Fig. 3a, b, 3c, 3d, 3e, 3f, 3g, 3h, 3i, and 3j conduct the flow behavior of stretching ratio number (c) involving the impacts of Blade, Brick, Cylinder, Platelets and Sphere shapes nanoparticles in view of *Cu* and TiO_2 nanoparticles. The stretching ratio number (c) is ration of stretching number in x-direction and stretching number in y-direction whereas flow of *Cu* and TiO_2 nanoparticles is depend upon values of (c). So, large values of (c) represents the more stretching the surface in both direction (horizontal) while more stretching of wall of the surface in view of direction (horizontal). Therefore, this more stretching ration in x-

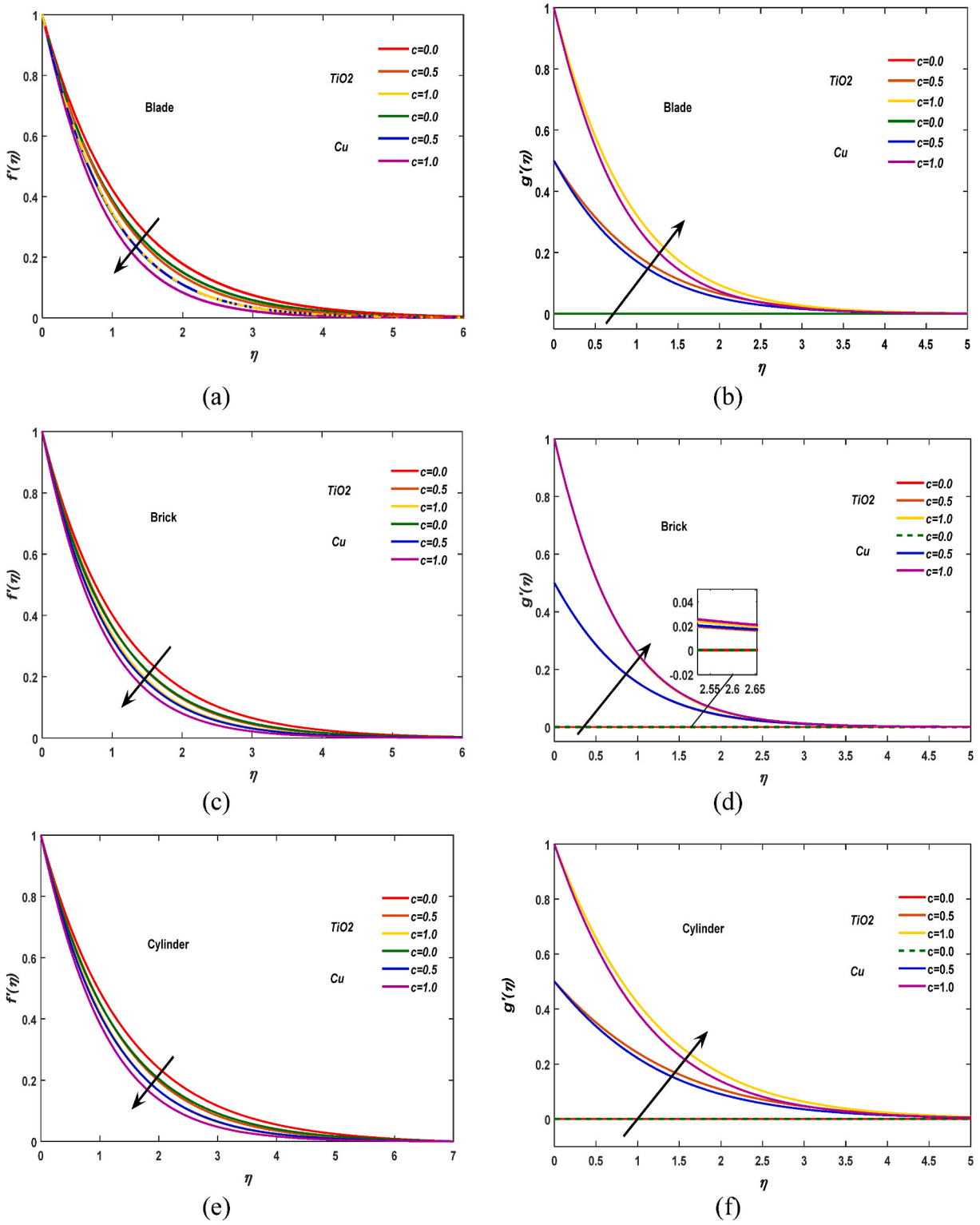

Fig. 3. (a–j). Variation of c on (f', g') by using various shape nanoparticales.

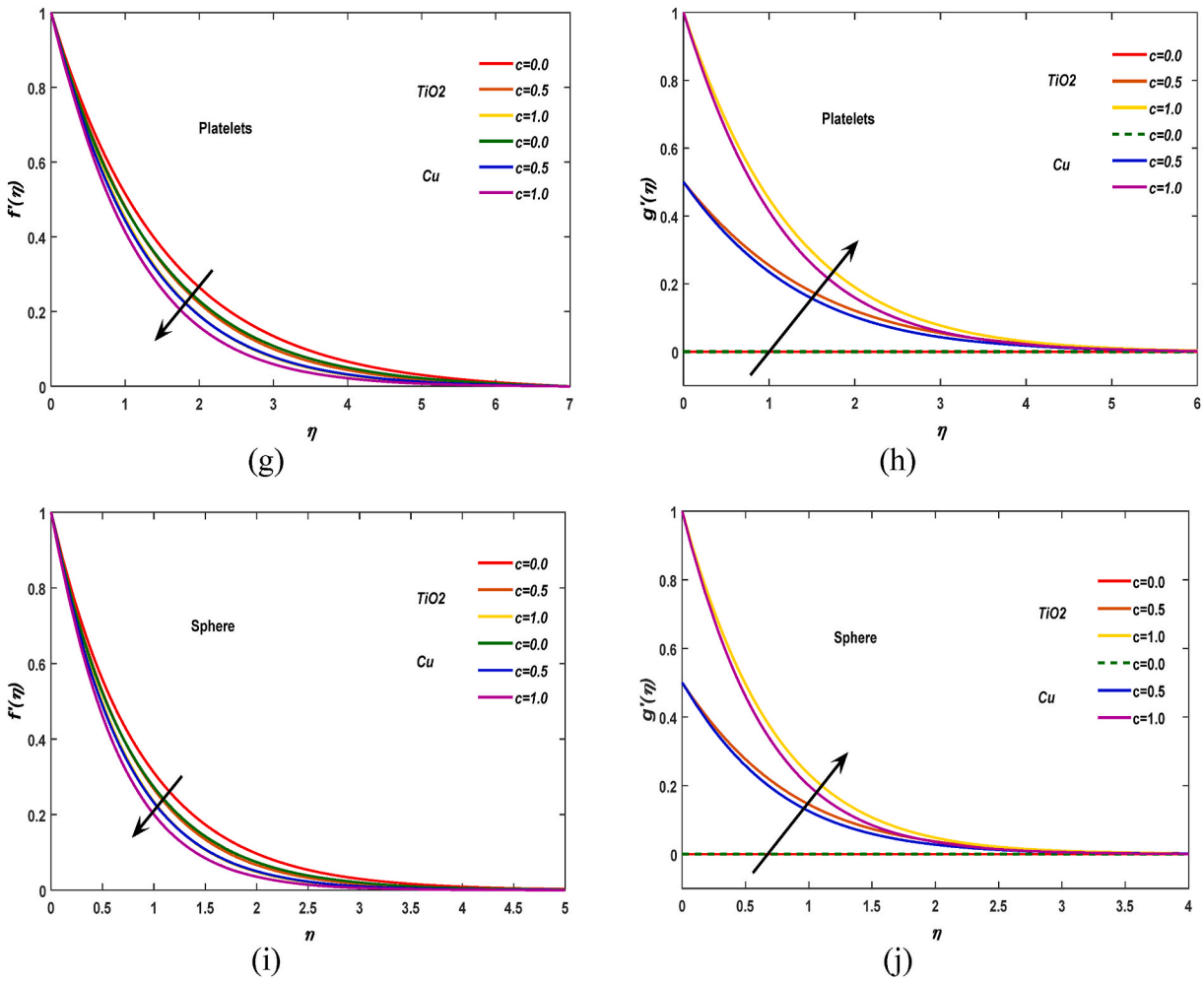

Fig. 3. (*continued*).

direction generates reduction in flow of *Cu* and TiO_2 by using different shapes of nanoparticles (Blade, Brick, Cylinder, Platelets and Sphere shapes). The vertical flow versus (*c*) in the presence of Blade, Brick, Cylinder, Platelets and Sphere shapes nanoparticles in view of *Cu* and TiO_2 nanoparticles is simulated by these graphs. From these figures, flow of *Cu* and TiO_2nanoparticles by using Blade, Brick, Cylinder, Platelets and Sphere shapes nanoparticles is enhanced due to large values of (*c*) because (*c*) having inverse relation versus stretching number in view of y-direction. So, flow of *Cu* and TiO_2nanoparticles using Blade, Brick, Cylinder, Platelets and Sphere shapes nanoparticles is reduced while flow behavior of TiO_2-nanofluid is higher than *Cu*-nanoparticles. Furthermore, thickness of MBL is reduced versus large values of (c) but thickness of MBL is enhanced against higher values of (c). The graphical assessments of volume fraction related to *Cu* and TiO_2nanoparticles in the presence of Blade, Brick, Cylinder, Platelets and Sphere shapes nanoparticles are conducted by Fig. 4a-j. The simulations from these figures are revealed that flow of *Cu* and TiO_2nanoparticles using Blade, Brick, Cylinder, Platelets and Sphere shape nanoparticles in x- and y-directions enhances using higher values of volume fraction number. It is also referred to that the role of (φ) on the flow of TiO_2nanoparticles higher than the velocity of *Cu* nanoparticles in the presence of Blade, Brick, Cylinder, Platelets and Sphere shapes nanoparticles.

Comparative study of TiO_2 and *Cu* in view of temperature field: The performance of various parameters called Prandtl and Eckert numbers on the role of thermal energy using several shapes of nanoparticles named as Blade, Brick, Cylinder, Platelets and Sphere shapes nanoparticles inserting the two kinds of *Cu* and TiO_2 nanoparticles (see Fig. 5a, b, 5c, 5d, 5e, 6a, 6b, 6c, 6d and 6e). The simulations of Prandtl number including Blade, Brick, Cylinder, Platelets and Sphere shapes nanoparticles in the presence of *Cu* and TiO_2 nanoparticles are performed by Fig. 5a, b, 5c, 5d, and 5e. The Prandtl number determines thermal performance inserting various shapes of nanoparticles called Blade, Brick, Cylinder, Platelets and Sphere including suspension of *Cu* and TiO_2nanoparticles while outcomes depict that heat energy is reduced due to enhancing the values of Prandtl number because according to definition of Prandtl number which is division of two layers MBL and TBL. So, inverse relation is investigated versus Prandtl number and TBL whereas large values of Prandtl number are not useful for enhancing the performance of heat energy. Physically, the variation in Prandtl number is suitable for MBL due to direct relation is investigated versus MBL whereas Prandtl number is not suitable against TBL. Moreover,

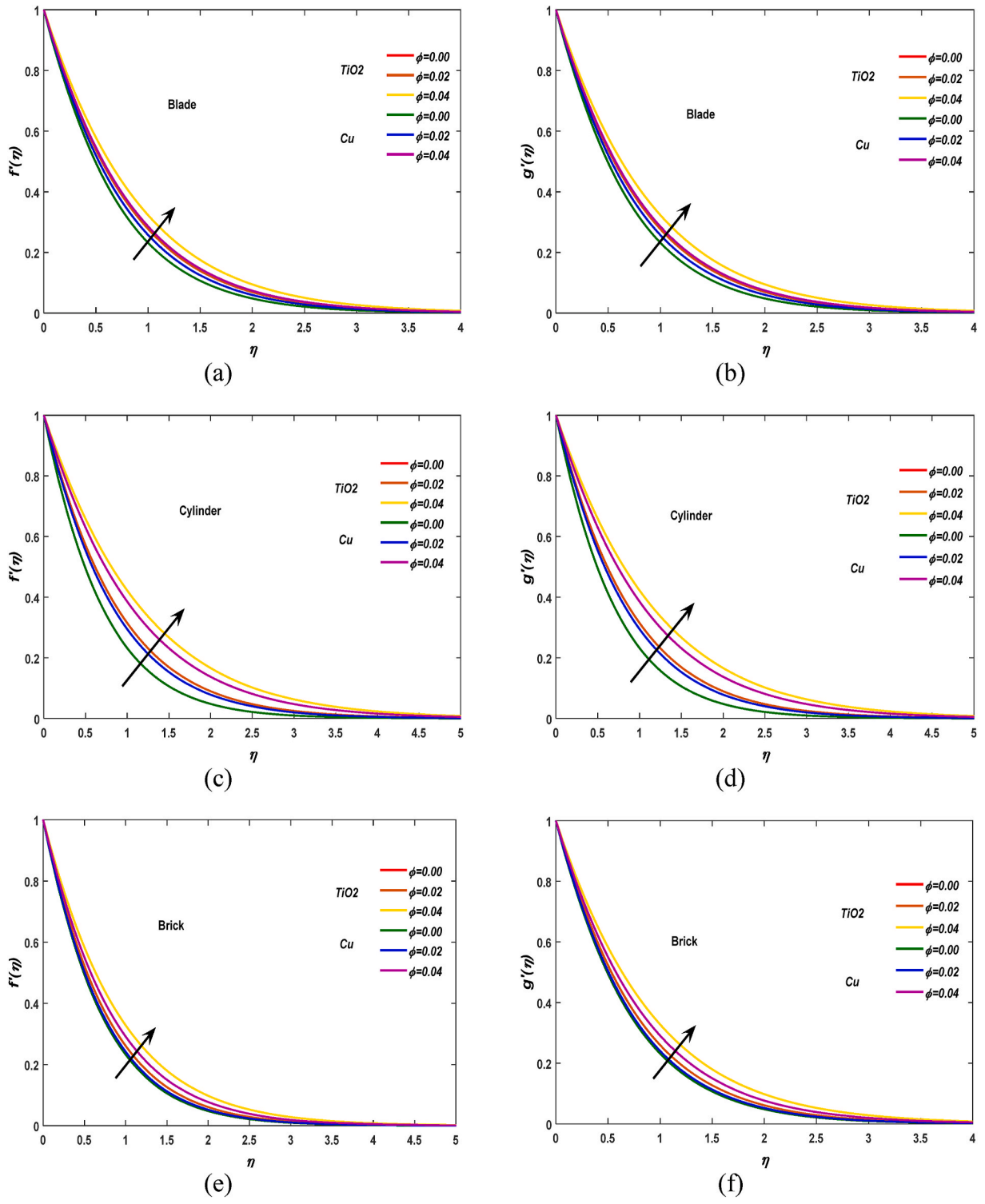

Fig. 4. (a–j). Variation of φ on $(f^{'}, g^{'})$ by using various shape nanoparticales.

Prandtl number has ability to control both layers (MBL and TBL) and performance of heat energy becomes enhance by adding TiO_2 nanoparticles as compare than thermal energy of *Cu* nanoparticles. Fig. 6a, b, 6c, 6d and 6e demonstrated the transfer of heat in view of *Cu* and TiO_2 nanoparticles using Blade, Brick, Cylinder, Platelets and Sphere shapes nanoparticles. It is demonstrated that from these

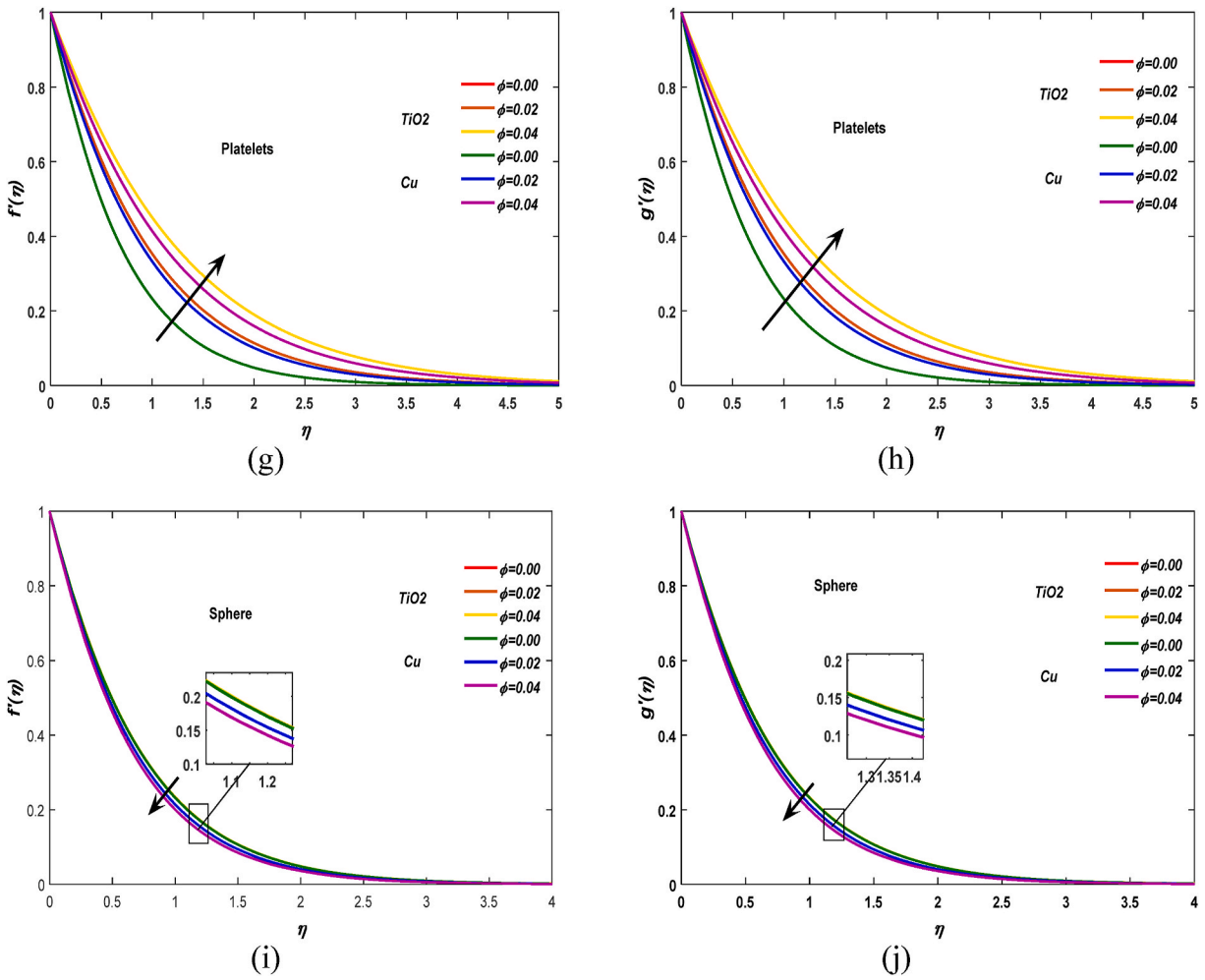

Fig. 4. (*continued*).

figures Eckert number reduces the heat energy in presence of Blade, Brick, Cylinder, Platelets and Sphere shapes nanoparticles. This reducing impact on layers of thermal boundary is developed due to viscous dissipation while thermal enhancement is determined more for the case of TiO_2 nanoparticles as compared for the case of *Cu* nanoparticles under the action of Blade, Brick, Cylinder, Platelets and Sphere shapes nanoparticles. It is also revealed that *Ec* having the inverse relation versus dissipation of heat energy. Therefore, large values of *Ec* generates less heat energy. Moreover, direct relation is found between viscous dissipation and heat energy. More heat energy is dissipated due to higher values of *Ec* because of this direct relation. So, more generation of heat energy is produced due to higher values of *Ec* number. An increasing graph of heat energy and *Ec* is plotted.

Simulations of temperature gradient and velocity gradient: The variation of Prandtl number and stretching ratio number on the temperature gradient and velocity gradient in the presence of Blade, Brick, Cylinder, Platelets and Sphere shapes nanoparticles including *Cu* and TiO_2 nanoparticles is conducted by Tables 3 and 4. From Table 3, it is demonstrated that divergent velocities in both directions (y-and x-direction) becomes speed up versus large values of stretching ratio number. Further, the comparative simulations of divergent velocities are conducted with published results of Khan et al. [20] in the absence of $M = 0$ and $\varphi = 0$. The temperature gradient is derived versus various values of Prandtl number in term of Blade, Brick, Cylinder, Platelets and Sphere shapes nanoparticles as well as two kind of nanoparticles called *Cu* and TiO_2 while these simulations are performed by Table 4. Table 4 illustrates an enhancement in Nusselt number against the large values of *Pr*. Moreover, simulations of Nusselt number is verified with published works.

5. Concluding observations

Transfer of heat energy in Newtonian fluid past a melting 3D surface with Blade, Brick, Cylinder, Platelets and Sphere shapes nanoparticles under the action of two kinds of nanoparticles called *Cu* and TiO_2 nanofluids is considered and generating model is solved by shooting approach. The numerical results of surface force and temperature gradient are addressed. These observations are

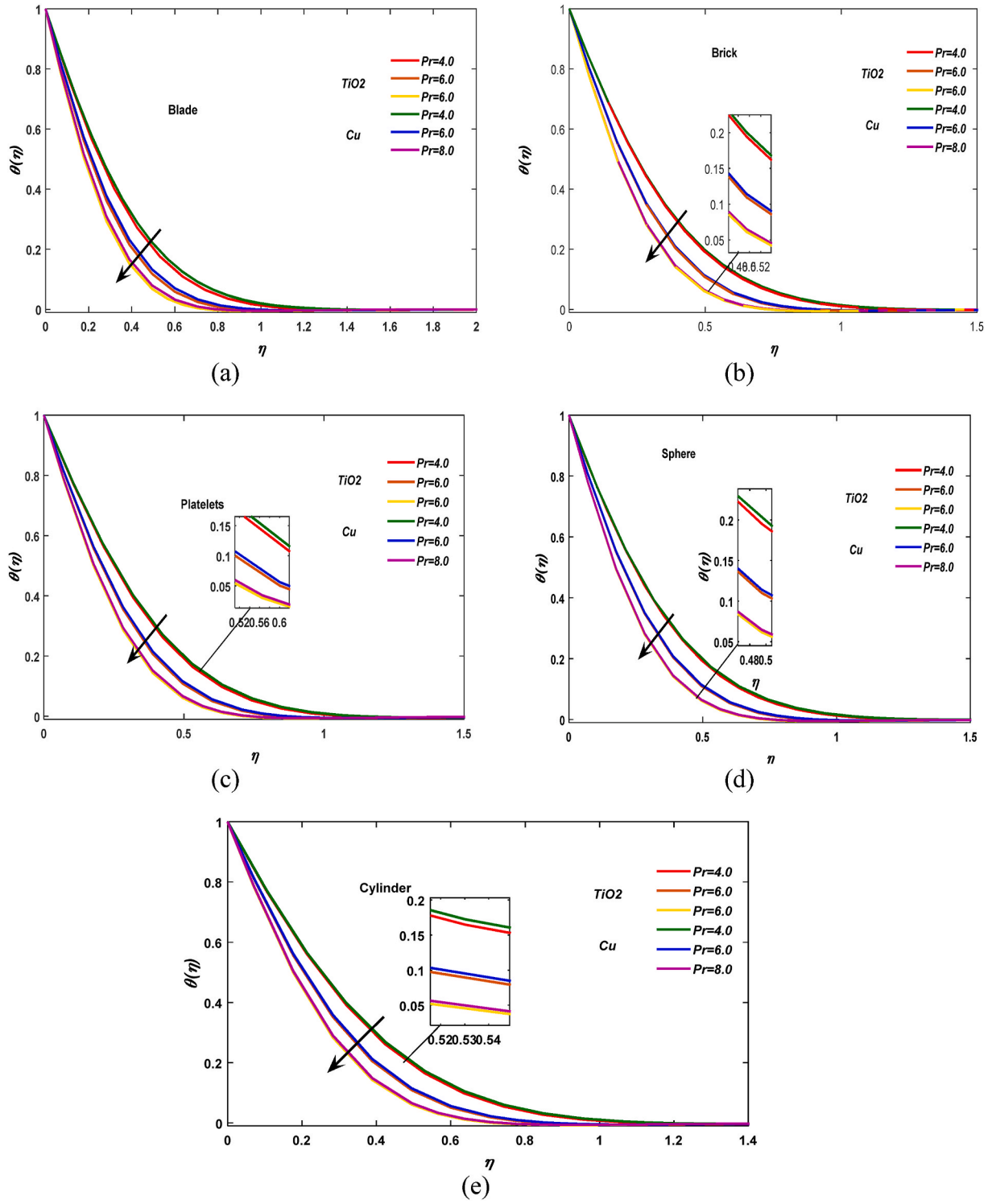

Fig. 5. (a–e). Variation of *Pr* on $\theta(\eta)$ by using different shapes nanoparticles.

summarized here:

- A reduction in thermal energy is noticed due to large values of *Pr* and *Ec*. Maximum production of heat energy is conducted as a higher for the case of TiO_2 nanoparticles rather than heat energy for the case of *Cu* nanoparticles;

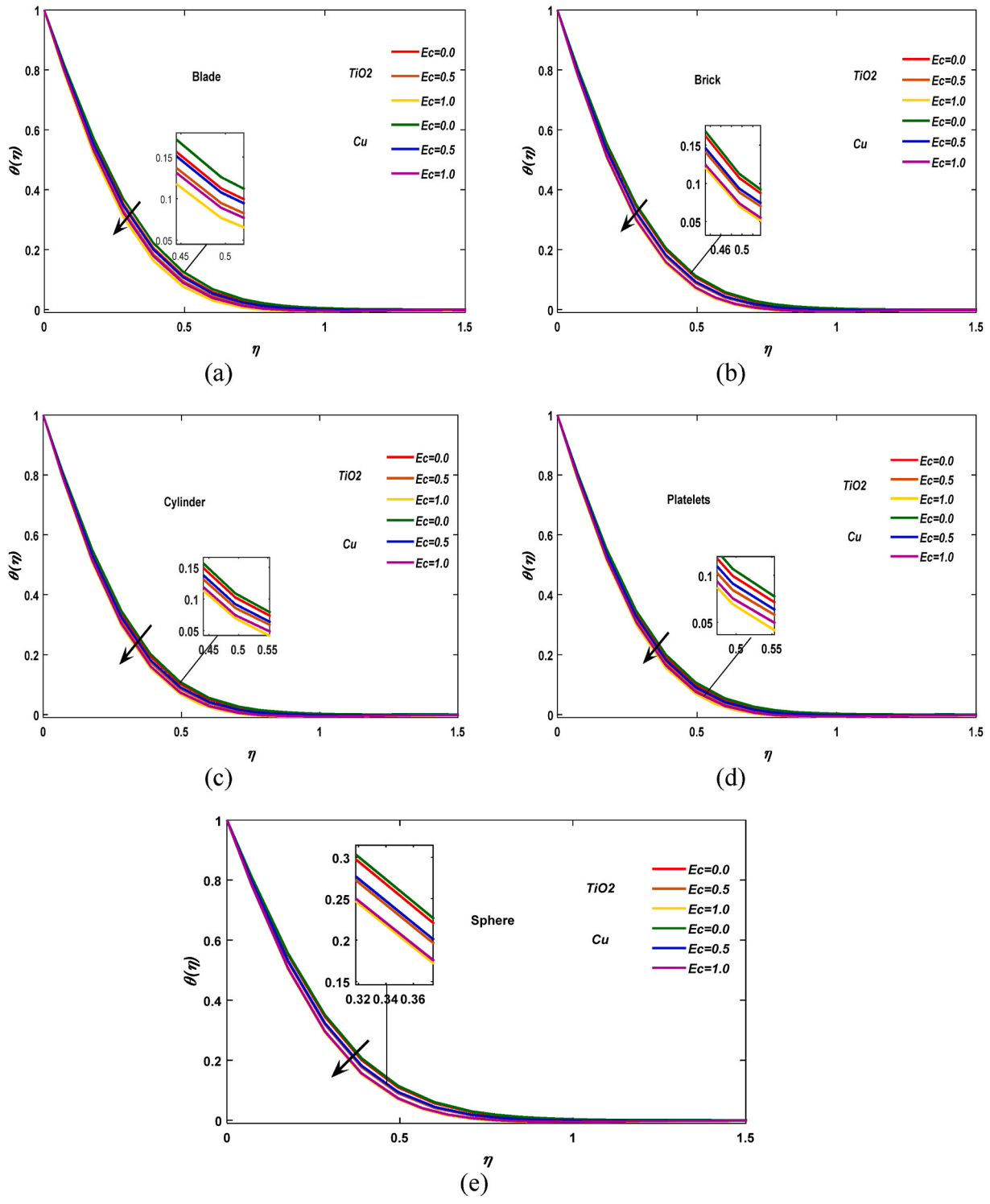

Fig. 6. (a–e). Variation of Ec on $\theta(\eta)$ by using numerous shape nanoparticles.

- Walls momentum diffuses slowly versus large values of Lorentz force but wall momentum in y-direction becomes more quickly diffuse by considering enhancement in stretching ration of the hot surface;
- Wall momentum is occurred less diffuse versus enhancement in stretching ration number;

Table 3
Comparative analysis for shear stresses.

n	c	$f''(0)$ Khan et al. [20]	Present	$g''(0)$ Khan et al. [20]	present
1	1.000000	1.000000	1.000000	0.000000	0.000000
	1.223961	1.223961	1.223965	0.6131010	0.6131012
	1.413927	1.413927	1.413925	1.414261	1.414260

Table 4
Comparison of values of reduced Nusselt number $-\theta(0)$ with the previous studies for $M = 0.4$, $k = 1.0, Ec = 1$, *and* $c = 1.0$.

Pr	Khan and Pop [26,27]	Makinde and Aziz [27]	Gorla and Sidawi [28]	Khan et al. [20]	Present
0.07	0.0663	0.0656	0.0656	0.06562	0.16712
0.20	0.1691	0.1691	0.1691	0.16909	0.87121
0.70	0.4539	0.4539	0.5349	0.45392	0.42730
2.00	0.9113	0.9114	0.9114	0.911360.87180	
7.00	1.8954	1.8954	1.8905	1.89542	1.85535
20.00	3.3539	3.3539	3.3539	3.35394	3.31423
70.00	6.4621	6.4622	6.4622	6.46231	6.42304

- Divergent velocities and temperate gradient are increased against higher values of Prandt and stretching ratio numbers. The Prandtl and Eckert numbers reduces heat energy.

Availability of data and material

The data used to support this study are included in the Manuscript.

Credit author statment

Tahir Naseem: Formal analysis; Software; Resources, Writing – review & editing. Umar Nazir: Software; Visualization; Formal analysis, Resources; Validation, Writing – review & editing. Muhammad Sohail: Conceptualization; Investigation; Writing – original draft; Supervision; Methodology; Software. Hussam Alrabaiah: Writing – review & editing; Software; Supervision El-Sayed M. Sherif: Software; Visualization; Formal analysis, Resources; Validation, Writing – review & editing. Choonkil Park: Project administration; Funding acquisition; Methodology; Visualization; Software; Writing – original draft.

Funding:

No external funding is available to report this study.

Authors' contributions

All the authors contributed equally.

Declaration of competing interest

The authors declare that they have no known competing financial interests or personal relationships that could have appeared to influence the work reported in this paper.

Acknowledgement

Researchers Supporting Project number (RSP-2021/33), King Saud University, Riyadh, Saudi Arabia. No external funding is available to report this study.

References

[1] S. Marzougui, F. Mebarek-Oudina, A. Assia, M. Magherbi, Z. Shah, K. Ramesh, Entropy generation on magneto-convective flow of copper–water nanofluid in a cavity with chamfers, J. Therm. Anal. Calorim. (2020) 1–12.
[2] M.S. Bhutta, S. Akram, P. Meng, J. Castellon, S. Agnel, H. Li, Y. Guo, G. Rasool, S. Hussain, M.T. Nazir, Steady-state conduction current performance for multilayer polyimide/SiO2 films, Polymers 13 (4) (2021) 640.
[3] U. Khan, A. Zaib, I. Khan, K.S. Nisar, Dual solutions of nanomaterial flow comprising titanium alloy (Ti 6 Al 4 V) suspended in Williamson fluid through a thin moving needle with nonlinear thermal radiation: stability scrutinization, Sci. Rep. 10 (1) (2020) 1–15.

[4] Z. Abdelmalek, U. Nazir, M. Nawaz, J. Alebraheem, A. Elmoasry, Double diffusion in Carreau liquid suspended with hybrid nanoparticles in the presence of heat generation and chemical reaction, Int. Commun. Heat Mass Tran. 119 (2020) 104932.
[5] H. Vaidya, K.V. Prasad, I. Tlili, O.D. Makinde, C. Rajashekhar, S.U. Khan, R. Kumar, D.L. Mahendra, Mixed convective nanofluid flow over a non linearly stretched Riga plate, Case Studies in Thermal Engineering 24 (2021) 100828.
[6] N.A. Shah, I.L. Animasaun, J.D. Chung, A. Wakif, F.I. Alao, C.S.K. Raju, Significance of nanoparticle's radius, heat flux due to concentration gradient, and mass flux due to temperature gradient: the case of Water conveying copper nanoparticles, Sci. Rep. 11 (1) (2021) 1–11.
[7] M. Nawaz, A. Elmoasry, J. Alebraheem, Impact of monocity and hybridity of nano-structures on thermal performance of micropolar fluid with novel heat flux theory: the Cattaneo–Christov heat flux theory, Journal of Materials Research and Technology 9 (4) (2020) 8618–8626.
[8] K.S. Nisar, U. Khan, A. Zaib, I. Khan, D. Baleanu, Numerical simulation of mixed convection squeezing flow of a hybrid nanofluid containing magnetized ferroparticles in 50%: 50% of ethylene glycol–water mixture base fluids between two disks with the presence of a non-linear thermal radiation heat flux, Frontiers in Chemistry *8* (2020).
[9] A. Shafiq, G. Rasool, C.M. Khalique, Significance of thermal slip and convective boundary conditions in three dimensional rotating Darcy-Forchheimer nanofluid flow, Symmetry 12 (5) (2020) 741.
[10] H. Waqas, U. Farooq, A. Ibrahim, Z. Shah, P. Kumam, Numerical Simulation for Bioconvectional Flow of Burger Nanofluid with Effects of Activation Energy and Exponential Heat Source/Sink over an Inclined Wall under the Swimming Microorganisms, 2021.
[11] M. Sohail, U. Nazir, Y.M. Chu, H. Alrabaiah, W. Al-Kouz, P. Thounthong, Computational exploration for radiative flow of Sutterby nanofluid with variable temperature-dependent thermal conductivity and diffusion coefficient, Open Phys. 18 (1) (2020) 1073–1083.
[12] A. Dawar, Z. Shah, P. Kumam, H. Alrabaiah, W. Khan, S. Islam, N. Shaheen, Chemically reactive MHD micropolar nanofluid flow with velocity slips and variable heat source/sink, Sci. Rep. 10 (1) (2020) 1–23.
[13] A. Aldabesh, M. Hussain, N. Khan, A. Riahi, S.U. Khan, I. Tlili, Thermal variable conductivity features in Buongiorno nanofluid model between parallel stretching disks: improving energy system efficiency, Case Studies in Thermal Engineering 23 (2021) 100820.
[14] M. Javed, N. Imran, A. Arooj, M. Sohail, Meta-analysis on homogeneous-heterogeneous reaction effects in a sinusoidal wavy curved channel, Chem. Phys. Lett. 763 (2021) 138200.
[15] R. Slimani, A. Aissa, F. Mebarek-Oudina, U. Khan, M. Sahnoun, A.J. Chamkha, M.A. Medebber, Natural convection analysis flow of Al2O3-Cu/water hybrid nanofluid in a porous conical enclosure subjected to the magnetic field, Eur. Phys. J. Appl. Phys. 92 (1) (2020) 10904.
[16] M. Zaydan, A. Wakif, I.L. Animasaun, U. Khan, D. Baleanu, R. Sehaqui, Significances of blowing and suction processes on the occurrence of thermo-magneto-convection phenomenon in a narrow nanofluidic medium: a revised Buongiorno's nanofluid model, Case Studies in Thermal Engineering 22 (2020) 100726.
[17] A. Shahzad, U. Gulistan, R. Ali, A. Iqbal, A.C. Benim, M. Kamran, S.U.D. Khan, S.U.D. Khan, A. Farooq, Numerical study of axisymmetric flow and heat transfer in a liquid film over an unsteady radially stretching surface, Math. Probl Eng. (2020), 2020.
[18] M. Sheikholeslami, S.A. Farshad, Z. Ebrahimpour, Z. Said, Recent progress on flat plate solar collectors and photovoltaic systems in the presence of nanofluid: a review, J. Clean. Prod. (2021) 126119.
[19] M. Sheikholeslami, S.A. Farshad, Z. Said, Analyzing entropy and thermal behavior of nanomaterial through solar collector involving new tapes, Int. Commun. Heat Mass Tran. 123 (2021) 105190.
[20] J.A. Khan, M. Mustafa, T. Hayat, M.A. Farooq, A. Alsaedi, S.J. Liao, On model for three-dimensional flow of nanofluid: an application to solar energy, J. Mol. Liq. 194 (2014) 41–47.
[21] M. Sohail, R. Naz, Modified heat and mass transmission models in the magnetohydrodynamic flow of Sutterby nanofluid in stretching cylinder, Phys. Stat. Mech. Appl. 549 (2020) 124088.
[22] S.I. Abdelsalam, M. Sohail, Numerical approach of variable thermophysical features of dissipated viscous nanofluid comprising gyrotactic micro-organisms, Pramana 94 (1) (2020) 1–12.
[23] N. Imran, M. Javed, M. Sohail, P. Thounthong, Z. Abdelmalek, Theoretical exploration of thermal transportation with chemical reactions for sutterby fluid model obeying peristaltic mechanism, Journal of Materials Research and Technology 9 (4) (2020) 7449–7459.
[24] N. Imran, M. Javed, M. Sohail, P. Thounthong, Z. Abdelmalek, Theoretical exploration of thermal transportation with chemical reactions for sutterby fluid model obeying peristaltic mechanism, Journal of Materials Research and Technology 9 (4) (2020) 7449–7459.
[25] M. Sohail, R. Raza, Analysis of radiative magneto nano pseudo-plastic material over three dimensional nonlinear stretched surface with passive control of mass flux and chemically responsive species, Multidiscip. Model. Mater. Struct. (2020).
[26] W.A. Khan, I. Pop, Boundary-layer flow of a nanofluid past a stretching sheet, Int. J. Heat Mass Tran. 53 (11–12) (2010) 2477–2483.
[27] O.D. Makinde, A. Aziz, Boundary layer flow of a nanofluid past a stretching sheet with a convective boundary condition, Int. J. Therm. Sci. 50 (7) (2011) 1326–1332.
[28] R.S.R. Gorla, I. Sidawi, Free convection on a vertical stretching surface with suction and blowing, Appl. Sci. Res. 52 (3) (1994) 247–257.